Journal of
Nanoscience and Nanotechnology
Vol. 5, 120–130, 2005

RESEARCH ARTICLE

Geometry and Topology of Diatom Shape and Surface Morphogenesis for Use in Applications of Nanotechnology

Janice L. Pappas*

Museum of Zoology, University of Michigan, 1109 Geddes Avenue, Ann Arbor, Michigan 48109-1079

Diatoms have attracted the interest of those involved in nanotechnology and the development of this discipline for research and practical application. These microorganisms exhibit self-assembly of silica on the micrometer scale, with parts of diatoms measuring on the nanometer scale. They exhibit a wide variety of shapes and patterns. An interest in diatom development and the geometry and topology of diatom shapes and gross patterns formed the focus of this study. Diatoms may be theoretically created on the basis of conic sections and quadratic surfaces expressed in parametric two-dimensional (2D) and three-dimensional (3D) functions (as sheets). Recreated diatom shapes, surfaces, and gross patterns based on 3D parametric equations are presented. Changes from one form to another are discussed as changes in magnitude or functional element within a given set of 3D equations for sequences that are phylogenetically or taxonomically related. Topological evolution and combinations of diatom shapes and surfaces are explored. An example shows how diatom forms depicted as 2-manifolds can be subjected to topological gluing to create a form whose surface is topologically different from the original. Topological surgery and gluing of diatoms as geometric forms may be useful in hypotheses about creating nanosubstrates and nanopatterned nanomaterials or in other applications of nanotechnology.

Keywords: 2-Manifold, Diatoms, Nanostructured Materials, Parametric Equations, Quadratic Surfaces, Theoretical Morphology, Topological Surgery.

1. INTRODUCTION

Recently, those interested in nanoscience have been paying attention to diatoms, one of the most exquisite groups of microorganisms because of their ability to exhibit three-dimensional (3D) self-assembly using silica.[1] Diatoms have characters reproducible on the micro-, meso-, and nanoscale, have existed since at least the Jurassic, and are abundantly present in Late Cretaceous and early Tertiary[2,3] as well as in Turonian, Campanian, and Maastrichtian deposits.[4] Diatoms exhibit a wide variety of shapes and surfaces that are amenable to quantification in relation to the geometric properties of their silica frustules (also known as valves).

The way in which diatoms reproduce and deposit silica to form their frustules may be related to concepts from geometry and topology as an approach to theoretical diatom morphogenesis. Aspects of, and mathematical hypotheses on, diatom morphogenesis may be useful in applications for creating nanomaterials for application in nanotechnology.

Three areas of background information are necessary in this connection: diatom morphogenesis and the geometry and topology of diatom forms. The following is a concise survey.

1.1. Diatom Ontogeny and Morphogenesis

Diatoms exhibit a multitude of shapes and patterns in their siliceous valve structure. Diatom shape is part of valve ontogeny[5] and is a result of many factors and interactions during valve morphogenesis.[6–9] Changes in valve shape may indicate approximate successive stages within a single species life cycle. Shape and form are directly inherited in diatoms as a result of auxospore formation and vegetative reproduction.[10] During vegetative reproduction, the parent

*Author to whom correspondence should be addressed.

 1533-4880/2005/5/120/011/$17.00+.25 doi:10.1166/jnn.2005.009

cell controls cell wall pattern formation. Species-specific patterned adhesions of the plasmalemma occur during pattern development.[11] The molding surface for the topography of the new valve is the cleavage furrow, which is shaped by turgor pressure, local contractions, and tension of the new membrane and cytoplasm while adhering to the cell wall. It is the cleavage furrow that is important in the adhesion of progeny cells to parent cells. The shape of the cleavage surface determines the shape of future valves.[8,9]

Ontogenetic studies are used to determine which shapes and structures are homologous and which developmental changes are necessary for morphogenesis. Characteristic modifications in shape that occur during postauxospore size reduction define the developmental trajectory in diatoms.[12] Slight differences between parent and daughter cells are genetic in nature but are translated through the diatom life cycle[13] as size reduction occurs.[12,14–16] Evolution from one morphological variant to another may be revealed by developmental changes. The developmental sequence is a basic attribute of genomic expression embodied in shape differences[17] as measurable morphological quantities.[18]

Size diminishes[12,14–16] over time and may continue for months or even years.[10,19] Size restoration occurs as a result of sexual reproduction. Auxospore populations range from the smallest specimens occurring at approximately 30–40% of the largest specimens.[20] In addition, if optimal environmental conditions are present, sexual reproduction should occur.[20] Diatom life cycles are approximately 2–40 years, but sexual reproductive activity may last only a few weeks.[19] This may explain the lack of observed auxosporulation in many diatom species.[19]

Shape restoration occurs as a result of two processes. First, contraction of the protoplast away from the cell wall occurs. Second, auxospore curvature with respect to the pervalvar axis determines valve shape. If the pervalvar axis is in the plane of curvature, initial valves are symmetrical where one is convex and the other is concave (e.g., *Achnanthidium*). If the pervalvar axis is perpendicular to the plane of curvature, initial valves will be laterally asymmetrical (e.g., *Cymbella*).[10] Frustule shape is adapted to withstand two opposing forces, i.e., turgor pressure internally can distend the cell wall, and shear stress from water currents exerts pressure externally.[9] In addition, this occurs as materials are exchanged such as ions, nutrients, and organic matter. Shape, size, and pattern changes will occur in tandem with the least amount of energy expended.[13,21]

Diatom symmetry is determined by the pattern formation center. In centric diatoms, an annulus (centrally located ring) is defined, followed by the formation of radially furcated ribs, which is then followed by silica deposition of the areolae.[22] In pennate diatoms with at least one raphe-bearing valve, the sequence of silica deposition events in pattern formation proceeds generally from sternum to raphe formation to silica deposition of the areolae.[22]

In pennate diatoms, the silicalemma is a membranous tube that expands laterally and runs the entire length of what will become the future valve, and this indicates the first appearance of the silica deposition vesicle[23] (SDV). During cleavage, the SDV is adjacent to the plasmalemma. The size of siliceous bands, hoops or plates of the perizonium controls the characteristic elongate shape of pennate diatoms.[10,9]

Developmental studies of silica deposition in araphid pennate diatoms have yielded some interesting preliminary results. In the early stages of development, some *Fragilaria* species may produce a series of annuli that next fuse to form a sternum during silica deposition.[22] In other araphid taxa, silica deposition is initiated in the area of the sternum, from which transapical ribs then develop, as in raphid pennate diatoms.[24] Eunotioid taxa may exhibit silica deposition whose developmental aspects are intermediate between raphid and araphid pennate diatoms.[6,22] Other patterns with regard to silica deposition include formation of Voigt discontinuities in *Cymbella*, *Encyonema*, and *Navicula* (sensu stricto)[25,26] or raphe position with respect to symmetry as in *Hantzschia* and *Nitzschia*.[27]

The general structure of the diatom cell wall may be described as two distinct parts. One is the valve face, as mentioned above. The other consists of the girdle bands (or epicingula and hypocingula) that is the site for cell division. The topography of the valve in girdle view is the valve mantle and is distinguishable from the morphology of girdle bands.[28]

Diatoms exhibit a number of forms and complexities. Generally, there are approximately 84 different kinds of diatom valve shapes, 20 different shaped pennate diatom valve ends, 57 different pennate diatom striae patterns, 59 different pennate diatom raphe and terminal fissure patterns and positions, 16 different sternum patterns in pennate diatoms, 21 different areolae patterns in centric diatoms, 38 different central area shapes/patterns, 18 costae, marginal structures and ocelli, 14 different valve elevation structures, 16 different valve undulation or torsional patterns, and 42 other structures, including septa, partecta, craticula, spines, setae, and rostra.[29] With the multitude of combinations of shapes and structures, it is no wonder that some have estimated the number of diatom species to be 10^6.[13]

This study does not intend to model diatom silica deposition exactly with respect to ontogeny and morphogenesis. Nor is the intent to describe theoretical diatom morphological evolution on the whole. My interest is in the many geometric shapes and surfaces that diatoms exhibit and the possibilities of evolving or combining shapes and surfaces for possible application in nanotechnological uses.

Theoretical changes in diatom surface and shape can be modeled by 3D parametric equations. Centric diatoms can be modeled using trigonometric or circular functions. For some pennate diatoms, combinations of parameterized

circular and hyperbolic functions are necessary to recreate their 2D surface or 3D form. Patterns on the valve surface have geometric form as well as the valve shape as a whole.[29] Gross changes in surface characters such as the sternum width and number of striae can be modeled. A series of shape changes can be used to show theoretical change in shape from a simple to a more complex form, and these changes may model sequences that depict taxonomically related taxa.

In this study, I want to devise and display theoretical diatoms as 3D geometrical forms or 2D surfaces (as sheets) in order to find at least one surface that resembles a diatom's valve face shape and gross surface. In addition, series of quantitative changes in sequences of theoretical forms are explored. These sequences will represent appropriate phylogenetic or taxonomic affinities of the forms depicted. Theoretical diatom forms or parts of these theoretical shapes and surfaces may be used in topological transformations to obtain newly assembled combinations of shapes and surfaces that might prove to be useful in nanotechnology. Knowledge about diatom geometry and topology may be useful in application for synthesizing materials where form controls function.

1.2. Geometry of Diatom Forms

In 2D, general valve shapes or forms consist of circular (centric diatoms) and rectilinear surfaces (pennate diatoms). These forms can be broken down geometrically into parts of conic sections. Centric diatom geometry is based on the circle. Pennate diatom geometry is not only based on the circle but also on the hyperbola. Hyperbolic elements of pennate diatom geometry are necessary to recreate the changes in curvature, sometimes over a short distance, on a given place on the valve edge. In addition, the entire valve outline curvature is bisymmetrical (or approximately so) and represented by a combination of circular and hyperbolic functions.

In 2D Euclidean space, R^2, circular functions are based on the identity $x^2+y^2=1$. In R^3, $x^2+y^2+z^2=1$ is the identity. In parametric form, the sphere is represented by $x=a\sin u$, $y=b\cos u$, and $z=v$.

In R^2, hyperbolic functions are based on the identity $\frac{x^2}{a^2}-\frac{y^2}{b^2}=1$. In R^3, the one-sheeted circular hyperboloid is $\frac{x^2}{a^2}+\frac{y^2}{a^2}-\frac{z^2}{c^2}=1$, and the one-sheeted elliptic hyperboloid is $\frac{x^2}{a^2}+\frac{y^2}{b^2}-\frac{z^2}{c^2}=1$ with respect to the z-axis. In parametric form, the hyperbola is represented by the identities $\cosh^2 x-\sinh^2=1$ or $\tanh^2 x+\operatorname{sech}^2 x=1$. The parametric representation of the one-sheeted circular hyperboloid is $x=a\sqrt{1+u^2}\cos v$, $y=a\sqrt{1+u^2}\sin v$, and $z=cu$. For the one-sheeted elliptic hyperboloid, the difference is in the y-equation where $y=b\sqrt{1+u^2}\sin v$. These identities form the basis for determining parametric forms and surfaces in R^n.

1.3. Parametric Equations and Diatom Forms as Surfaces

Parametric equations are one way to represent curves as surfaces. By using parameters, coordinates may be separated independently of one another to provide flexibility in controlling the shape of curves. In addition, direct transformations of the equations may be used. Generally, parametric representations are not unique in that more than one parameterization can be created for a given curve. However, they are useful for the purpose of representing change in shape within a sequence of related forms, and in this case, the diatom sequences to be parameterized and displayed are indicative of approximate phylogenies or taxonomically related forms.

All parameterized surfaces created for the purpose of this study are quadratic surfaces. These surfaces may be ruled or doubly ruled. Parameterization of certain basic geometric forms, or combinations of them, is useful in representing theoretical diatom shapes and surfaces. Examples of these basic forms include one-sheeted elliptic hyperboloids (ruled surface) and hyperbolic paraboloids (doubly ruled surface). Surface variation by rotation and/or twisting of a ruled or doubly ruled quadratic surface allows for representation of gross changes in diatom pattern within a sequence.

1.4. Topology of Diatom Forms

Previously, the concern has been about the relation between diatom shape and parameterized circular and hyperbolic functions and their depiction geometrically. At present, attention focuses on transformation of shapes among diatoms. This involves topology,[30] including the study of deformations in space.

All diatoms have the same topology. Their forms are deformations of a ball. Manifolds are a class of topological spaces that establish an equivalence among diatom forms. Although all diatoms are topologically equivalent, most are geometrically different. They are 2-manifolds in Euclidean R^3 space. A diatom in valve view looks like a 2D surface, although it actually curves back around itself to the other valve. Locally, in the neighborhood of a point, manifolds look like Euclidean spaces. For every point on a diatom, there is a neighborhood that is the open unit ball and is equivalent to a Euclidean space. Globally, diatoms are 3D objects in a 3D world. Manifolds are classified by the genus, which is defined as the number of holes they have.

Defining diatoms as 2-manifolds is useful because of the properties manifolds have as topological spaces. Manifolds of the same class can be transformed with a simple condition being met. If the manifold is cut, the "ends" would need to be glued back together to preserve this topological space as the same class of manifold. If a diatom was arbitrarily cut, then twisted and knotted, and

then had its ends glued back together, the new shape would be topologically equivalent to the original diatom. If two different diatoms were cut, twisted, and knotted, then had the ends of one diatom glued to the ends of the other, the resultant shape would be topologically equivalent to either of the two original diatoms, provided that the number of holes from original to created form remains the same. In other words, one diatom segment could not be parameterized in a different direction if the genus or number of holes is to be preserved. The cutting of manifolds is termed topological surgery. Manifolds representing diatoms are homeomorphic, since they are continuous, invertible mappings of one another, regardless of the dimensionality of space in which they are embedded. Diatoms are compact 2-manifolds since they are metric spaces, they have boundaries, and they are orientable.

In order to recreate diatom shapes using topological surgery or gluing, a surface grid or mesh can be used. In topological transformations, surgery occurs at those points were topological change occurs. Topological characteristics of diatom forms are important in order to maintain the desired properties of the diatoms while they undergo transformation.

2. METHODS

Diatoms shapes were created using 3D parametric equations, starting with combinations of circular functions. Changes to combinations of circular and hyperbolic functions along the x-, y-, or z-axis were used to create noncircular forms. The surface of each geometric figure was incrementally changed with respect to one and/or the other parameter used. The resultant combinations of functions were displayed in graphical form. Geometric representations were displayed in sequences such that changes from one form to another were documented by changes in magnitude or function from one set to the next set of 3D parametric equations for each form created. Each sequence represents approximate diatoms taxa forms that are related in a phylogenetic sense.

Diatoms created from 3D geometric representation were used as 2-manifolds so that new topological spaces could be created. In some cases, topological surgery and gluing was used on one 2-manifold to change the geometry. In other cases, topological surgery and gluing was used to create new combinations of diatom valve parts from different diatoms. A control mesh or grid that was used in creating theoretical geometric forms and surfaces was used to map topological changes for a given diatom. Between diatoms, transformation from original form to the new form was mapped as a correspondence from one diatom to another using a grid. One example of topological changes was displayed as a sequence of the morphing and evolution of surfaces.

Fig. 1. Bilobate[29] diatom form, wide and short.

3. RESULTS

3.1. Geometry

One sequence of created pennate diatom shapes with gross surfaces was created for eunotioid and bilobate taxa (Figs. 1–5). Parametric equations for Figure 1 were

$$x = \sin t^4 * 130\cos u + \cos t^3 * 6\sin u^2 \quad (1)$$

$$y = 30\text{sech}\,\frac{t}{64} * \tanh u - \tanh t * \sin u \quad (2)$$

$$z = 20\sin t^4 * \tanh u^4 + \cos t^3 * \tanh u^3 \quad (3)$$

where $t = (\frac{-\pi}{2}, \frac{\pi}{2})$, $dt = \frac{\pi}{4}$, $u = (\frac{-5\pi}{8}, \frac{5\pi}{8})$, and $du = \frac{\pi}{70}$. One deformation of this parametric surface is displayed in Figure 2. The equations were the same as those for Figure 1 except for three changes. In the x-equation for Figure 2, the first cosine term was multiplied by 60 rather than by 130. In the y-equation, the hyperbolic secant term was multiplied by 50 instead of 30. In the z-equation, the sine term was multiplied by 8 rather than 20.

Figure 3 was changed even more. In the x-equation, the first cosine term was multiplied by 30, and the last sine term was multiplied by 10. In the y-equation, the last two terms that were multiplied together, were eliminated, and the hyperbolic tangent term was multiplied by 0.7. In the z-equation, the last two terms multiplied together were eliminated, the sine term was multiplied by 8, and the hyperbolic tangent term was multiplied by 2. Figure 4 had changes to all three equations as well. The first cosine term was multiplied by 25 and the last sine term was multiplied by 6 in the x-equation. The hyperbolic tangent term in the y-equation was multiplied by 1. The z-equation was more similar to that for Figures 1 and 2. The cosine and hyperbolic tangent terms that were multiplied together were added to the first two terms in the z-equation.

Figure 5 resembled *Eunotia flexuosa*[31] with the x-equation changed from what was given for Figure 4. The last two terms multiplied together then added to the first product had been eliminated, with $t = (\frac{-\pi}{4}, \frac{\pi}{2})$ and $u = (\frac{-5\pi}{8}, \frac{5\pi}{8})$, while dt and du remained the same.

Another sequence of pennate diatom shapes with gross surface features was created to look like naviculoid taxa

Fig. 2. Bilobate[29] diatom form, more elongated than in Figure 1 and slightly transapically asymmetrical.

RESEARCH ARTICLE

Fig. 3. Bilobate[29] diatom form, narrower in the mid-valve region than that for Figure 2.

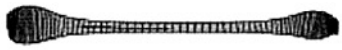

Fig. 4. Bilobate[29] diatom form, even narrower than in Figure 3 and transapically asymmetrical.

Fig. 5. *Eunotia flexuosa*[29] form.

Fig. 6. Naviculoid form, rhombic.[29]

Fig. 7. Naviculoid form, lanceolate.[29]

Fig. 8. Naviculoid form, acicular to fusiform lanceolate.[29]

Fig. 9. Naviculoid form, lanceolate with cuneate ends.[29]

(Figures 6–11). For Figure 6, the parametric equations were

$$x = 3\sin\frac{t}{2} \tag{4}$$

$$y = 0.5\text{sech}\, t * \tanh 10u \tag{5}$$

$$z = \sin\frac{t}{2} \tag{6}$$

where $t = (-\pi, \pi)$, $dt = \frac{\pi}{32}$, $u = (-2\pi, 2\pi)$, and $du = \frac{\pi}{8}$. The only change from Figure 6 to Figure 7 was 0.3 multiplied by the hyperbolic secant term rather than 0.5 in the y-equation, and $dt = \frac{\pi}{64}$ to reflect finer striae. Figure 8 was changed from Figure 7 in the x-equation where the sine term was multiplied by 4 rather than by 3. For Figure 9, the x-equation was the same as it was for Figures 6 and 7, but the y-equation was changed to be

$$y = 3\,\text{sech}\, 1.2t * \tanh 10u \tag{7}$$

and $dt = \frac{\pi}{16}$ to reflect coarser striae. Figure 10 was different from Figure 9 in that the hyperbolic secant term in the y-equation was multiplied by 1 rather than by 3 and the z-equation was changed to be $z = \sin\frac{t}{16}$. The parametric equations for Figure 11 were the same as those for Figure 10 with the exception that the z-equation was the same as was given for Figures 6–9.

Related to the naviculoid sequence was the gomphonemoid sequence of figures. Figure 12 was used as a way to make the transition from a naviculoid shape to a gomphonemoid shape. The parametric equations for Figure 12 were the same as those for Figure 11 except in the z-equation, the tangent function replaces the sine function. In the rest of the gomphonemoid sequence, the changes were small. For Figure 13 the cosine function replaced the tangent function in the z-equation. Figure 14 depicted the same equations as those for Figure 13, with the exception that in the z-equation, $\frac{t}{2}$ was replaced by t.

Fig. 10. Naviculoid form, rhombic,[29] but shorter than in Figure 6.

Fig. 11. Naviculoid form, rhombic to quadrate.[29]

Fig. 12. Transitional form, central area protruding with drawn out ends.

Fig. 13. Gomphonemoid form, somewhat hastate.[29]

Fig. 14. Gomphonemoid form, clavate with a narrow cuneate head pole.[29]

Fig. 15. Gomphonemoid form, clavate with an apiculate and produced head pole.[29]

In the x-equation for Figure 15, $\frac{t}{2}$ was replaced by $\frac{t}{3}$, and for Figure 16, $\frac{t}{2}$ was replaced by $\frac{t}{4}$.

Another variation on the naviculoid form is depicted in Figure 17. When compared to Figure 12, the parametric equations for Figure 17 were different in that the tangent function was used instead of the sine function in the x-equation. In addition, for Figure 17, the hyperbolic secant term was multiplied by 2 rather than by 0.5 as it was in the y-equation for Figure 12. The z-equation was the same for both figures.

Figure 18 has been given a "twist" when compared to Figure 17. The parametric equations for Figure 18 were

$$x = 4\tan\frac{t}{2} + \sin u \tag{8}$$

$$y = \operatorname{sech} t * 3\tanh u \tag{9}$$

$$z = \sin\frac{t}{2} * \cos\frac{u}{2} \tag{10}$$

where $t = (-\pi, \pi)$, $dt = \frac{\pi}{16}$, $u = (-\pi, \pi)$, and $du = \frac{\pi}{8}$. This figure is a transition to an *Actinella*[31]-like form depicted in Figure 19. The changes were in the y-equation, where $\frac{u}{2}$ was used with respect to the hyperbolic tangent function, and the z-equation was

$$z = \sin\left(\frac{t}{2} - 1\right) * \cos\frac{u}{2} \tag{11}$$

where $t = (-\pi, \frac{\pi}{2})$.

A number of other forms were created to display different diatom shapes and surfaces. Figure 20 resembles

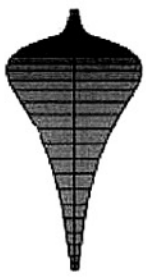

Fig. 16. Gomphonemoid form, clavate with a more apiculate and produced head pole[29] than that for Figure 15.

Fig. 17. Transitional form, small central area protrusion with longer drawn out ends than that for Figure 12.

Fig. 18. Transitional form from Figure 17 with the grid surface "twisted."

Fig. 19. *Actinella*[31]-like form.

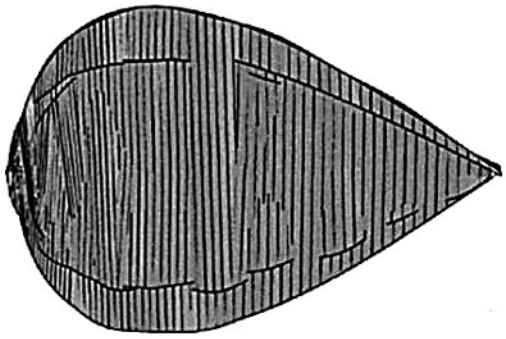

Fig. 20. *Surirella peisonis*[32] form.

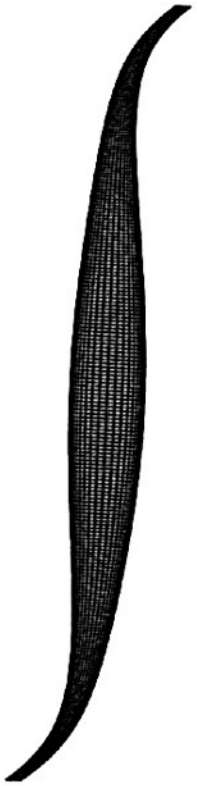

Fig. 21. *Gyrosigma*[33] form.

Surirella peisonis.[32] Parametric equations used to create this form were

$$x = \sin t^4 \cos u^2 \tag{12}$$

$$y = 2\cos\frac{t}{8} * \sin\frac{u}{2} \tag{13}$$

$$z = \sin t^3 \sin u \tag{14}$$

where $t = (\frac{-\pi}{2}, \pi)$, $dt = \frac{\pi}{4}$, $u = (0, 2\pi)$, and $du = \frac{\pi}{70}$.

Figure 21 resembles Gyrosigma,[33] with a grid depicting the valve surface. This form and pattern were produced

by parametric equations

$$x = \tan(t/2) \tag{15}$$

$$y = \operatorname{sech} 0.8t \tanh 20u + \cos\frac{t}{4} \tag{16}$$

$$z = \sin t + 3t \tag{17}$$

where $t = (-\pi, \pi)$, $dt = \frac{\pi}{128}$, $u = (-2\pi, 2\pi)$, and $du = \frac{\pi}{300}$.

One way to depict the sternum that looks like *Diploneis*[34] is presented in Figure 22. The parametric equations for this form were

$$x = \sin t * \tanh u \tag{18}$$

$$y = \cos t * \tanh 8u \tag{19}$$

$$z = \sin t * \tanh u \tag{20}$$

where the intervals for the parameters and incremental changes were $t = (0, 2\pi)$, $dt = \frac{\pi}{20}$, $u = (\frac{-\pi}{2}, \frac{\pi}{2})$, and $du = \frac{\pi}{20}$.

A series of figures were created to show changes in sternum width or a central line present to indicate a raphe. Figures 23 and 24 show araphid-like forms, while Figures 25 and 26 show raphid-like forms. The parametric equations for all these figures differed in magnitude changes either in one equation or incrementally with respect to a parameter. For Figures 23 and 25, the parametric equations were

$$x = \sin t^3 * \cos u \tag{21}$$

$$y = 4\cos\frac{t}{8} * \cos u \tag{22}$$

$$z = \sin t^2 * \sin u \tag{23}$$

where $t = (\frac{-\pi}{2}, \frac{\pi}{2})$, $dt = \frac{\pi}{5}$, $u = (\frac{-\pi}{2}, 2\pi)$, and $du = \frac{\pi}{50}$ for Figure 23. Parameters t and u are the same, but $dt = \frac{\pi}{4}$ and $du = \frac{\pi}{70}$ for Figure 25. For Figures 24 and 26, the parametric equations differed from those for Figures 23 and 25 in only the y-equation. In this equation, the first cosine term is multiplied by 2 rather than 4. The intervals for parameters t and u associated with Figures 24 and 26 were the same as they were for Figures 23 and 25. The incremental change of dt and du for Figure 24 is the same as that for Figure 23. Figures 25 and 26 had the same values for incremental change of dt and du.

3.2. Topology

To illustrate topological surgery and gluing,[35] a series of surface morphings was devised and displayed. One example is the sequence in Figure 27. To start, a theoretical 3D *Eunotia*[31] has been created. In the next two deformations, the *Eunotia*[31] is bent, then flattened. In the fourth deformation step, the bend is increased such that the flattened surface becomes horseshoe-shaped. Subsequently,

Fig. 22. *Diploneis*[34] form.

Fig. 23. Narrow pennate diatom valve form with a narrow sternum.

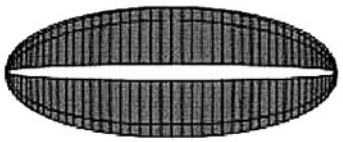

Fig. 24. Wider pennate diatom valve form with a wider sternum.

Fig. 25. Narrow pennate diatom valve form with "line" as raphe, parallel striae.

Fig. 26. Wider pennate diatom valve form with "line" as raphe, parallel striae.

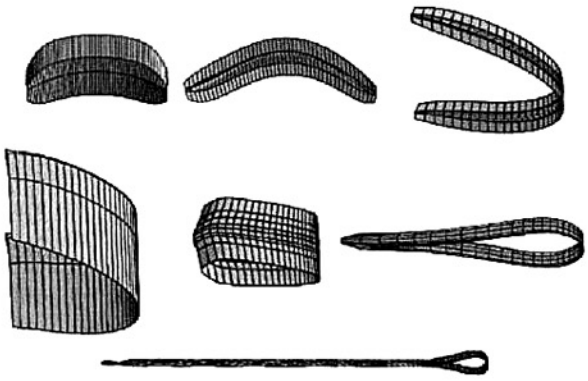

Fig. 27. An example of topological morphing using a 3D *Eunotia*[31] form. Subsequent deformations are bending to more bending and flattening the surface to stretching into a "sheet" to gluing the ends of the sheet together, to elongating the glued sheet to stretching to an *Asterionella*[31]-like form that is topologically different from the original form.

a ring is created, making a topological surface of a different genus. Elongation of the ring and tapering one end produces the next deformation. Further elongation of the surface produces an *Asterionella*[31]-like form, but the head pole has a hole in it. The final surface is topologically different from the original surface, and this shows one example of how topological evolution of surfaces may occur.

4. DISCUSSION

The results of this study provide ideas for the potential combination of forms available from diatoms, albeit on a theoretical basis. Silica deposition determines diatom valve morphology, which is largely a part of the genetic process.[5,9]

Using 3D parametric equations based on circular and hyperbolic functions, diatom forms may be created whereby at least one of the surfaces (a sheet) resembles the valve face in shape and gross surface pattern. These theoretical diatoms may form the basis of potential combinations and recombinations of diatoms or parts of diatoms in the creation of nanomaterials.

Suppose you needed a particular combination of 3D shapes or 2D surfaces for a nanosubstrate to be used in some sort of a nanodelivery system or for use in combination with a thin film. If you could culture the diatom shapes and surfaces you need, then do "nanosurgery" and "nanogluing" to piece these together just as was done using diatom forms as 2-manifolds in topology, you could potentially create any shaped surface imaginable. Alternatively, perhaps cultured diatoms could be genetically modified to produce parts that could be harvested and "nanoglued" together, or the diatoms themselves could be "nanoglued" together, then perhaps parts or slices of the new form could be used.

Diatoms react to their environment such that their morphology can be manipulated within an artificial setting. Culturing diatoms in closed vesicles has produced aberrant forms. That is, nutrient or ion imbalances as well as temperature and light conditions have produced abnormalities in diatom shape and valve structure in the laboratory.[36] Mathematically morphing diatom shape or surface may be useful in developing desired manipulation of diatom shape or pattern in conjunction with culturing diatoms to produce desirable nanostructured materials.

We know to some degree about the way in which diatoms deposit silica and how they morphogenetically develop. By creating theoretical diatoms based on geometry and morphing them based on topology, a combination of developmental and mathematically tailored diatoms may be useful in hypothesizing about possibly useful nanomaterials. During mitosis, the first indication of cell division occurs during metaphase. Subsequently, there is a pause, then division resumes during anaphase.[37] Perhaps division may be thought of as "topological surgery" during development. Adhesion of progeny to parent cell is sort of a "topological gluing" in principle that might be applied to nanogluing diatoms or parts of them to one another.

Pattern formation of centric and pennate diatoms may be viewed as types of topological deformations. Perhaps developmental changes with respect to silica deposition could produce centric diatoms with holes in the middle like a torus. Parts of such diatoms could be useful as nanostructures. Silica deposition and lateral expansion in pennate diatoms is another type of topological deformation. For some araphid diatoms where annuli fuse to create a sternum during silica deposition, this process could be construed to be topological gluing of circular forms to evolve into an elongated more rectilinear form or a combination of topological spaces whereby the manifold class remains the same.

In theoretical morphogenesis of surfaces and forms, geometrical and topological properties proved to be an interesting preliminary way to consider the possible flexibility of using diatoms in nanotechnology. The results of this study may have potential use in connection with modified nanofabrication of diatom silica[38] for nanopatterned materials, among various nanosubstrates and nanostructured materials.[39] Given the physical and mechanical properties of diatoms as durable structures,[40,41] combinations of diatoms or their parts may prove to be quite useful in nanotechnology. With interest in fields such as object recognition[42] and animation,[35] ways to devise theoretical surfaces are evident in current research. Other methods to model surfaces include using B-splines and a control mesh,[43] free-form deformation of a flattened parameterized Beziér surface with a grid,[44] implicit surface deformation,[45] and curvilinear coordinate surface mesh generation using the Cummings model.[46] Perhaps one or all of these methods may be useful in application of diatoms as nanomaterials as well.

In this study, diatoms or parts of diatoms may be viewed as geometrical constructs and topological surfaces or structures. Recombining such surfaces and structures can be accomplished mathematically and may show promise in using diatoms in applications of nanotechnology.

GLOSSARY

Adhesions patterned areas where the plasmalemma is attached to the cell wall.

Annulus central ring on the cell wall surface of centric diatoms.

Araphid a pennate diatom that does not have a raphe.

Areolae pores on the cell wall surface of diatom valves.

Auxospore a specialized cell produced after sexual reproduction that enables a diatom to restore its size after asexual (vegetative) reproduction.

Cingulum a girdle band.

Centric round diatoms with radial ribs.

Cleavage furrow an incision appearing around the periphery of the cell wall while nuclear division occurs.

Costae ribs on the cell wall surface of diatom valves.

Craticula internal ribs that are interconnected in a grid-like pattern within valves.

Epicingulum a girdle element associated with the older valve of a diatom.

Eunotioid pennate diatoms that are shaped and have cell wall surface characteristics like the genera *Eunotia*, *Peronia*, and *Amphicampa*.

Frustule the valve of a diatom consisting of the valve face and valve mantle.

Furcated ribs branching ribs on the cell wall surface of centric diatoms.

Initial valves valves formed after completion of auxospore expansion.

Hypocingulum a girdle element associated with the newer valve of a diatom.

Partecta internal chambers of the cingulum next to the valve mantle.

Pennate elongated diatoms with ribs extending approximately perpendicular to a central, elongated axis.

Perizonium a hoop of silica deposited during auxospore expansion.

Pervalvar axis in the plane that bisects a diatom parallel to its girdle bands or valve face.

Plasmalemma plasma membrane created during cleavage that molds the siliceous part of the cell wall.

Protoplast cellular contents of a diatom that have internally contracted from the cell wall.

Raphe longitudinal slits in a central, elongated area (sternum) on the cell wall surface of pennate diatoms.

Rostra long, thin projection on the ends of pennate diatom valves.

Septa an internal structure extending from the cingulum into the internal part of a valve.

Setae bristles or hairlike projections of valves.

Silica deposition vesicle (or SDV) a membranous vessel attached to the plasmalemma where silica condensation occurs.

Silicalemma the membrane of the silica deposition vesicle.

Spines long, hair-like projections of valves.

Sternum a central elongated area on the cell wall surface of pennate diatoms.

Striae lines of pores on diatom valves.

Transapical ribs ribs extending approximately perpendicular to a central, elongated axis on the cell wall surface of pennate diatoms.

Valve the cell wall of a diatom; also known as a frustule.

Voigt discontinuities faults that develop in striae patterns in some pennate diatoms.

Acknowledgments: The author expresses gratitude for the helpful comments of R. Gordon, F. A. S. Sterrenburg, D. Raup, and P. Rosin.

References and Notes

1. J. Parkinson and R. Gordon, Beyond micromachining: The potential of diatoms. *Trends Biotechnol.* 17, 190 **(1999)**.
2. D. M. Harwood and R. Gersonde, 26. Lower cretaceous diatoms from ODP Let 113 Site 693 (Weddell Sea). Part 2: Resting spores, chrysophycean cycstes, an endoskeletal dinoflagellate, and notes on the origin of diatoms. *Proc. Ocean Drill. Program: Sci. Results* 113, 403 **(1990)**.
3. D. M. Harwood and V. A. Nikolaev, Cretaceous diatoms: Morphology, taxonomy, biostratigraphy. In *Siliceous Microfossils*, edited by D. Blome and co-workers, Paleontological Society short Courses in Paleontology **(1995)**, Vol. 8, p. 81.
4. N. I. Strelnikova, Diatoms of the cretaceous period. *Beih. Nova Hedwigia* 53, 311 **(1975)**.
5. D. G. Mann, An ontogenetic approach to diatom systematics, in *Proceedings of the Seventh International Diatom Symposium*, edited by D. G. Mann, O. Koeltz, Koenigstein **(1984)**, p. 113.
6. A.-M. M. Schmid and D. Schulz, Wall morphogenesis in diatoms: Deposition of silica by cytoplasmic vesicles. *Protoplasma* 100, 267 **(1979)**.
7. A.-M. M. Schmid, Valve morphogenesis in diatoms: A pattern-related filamentous system in pennates and the effect of APM, colchicine and osmotic pressure. *Nova Hedwigia* 33, 811 **(1980)**.
8. A-M. M. Schmid, Morphogenetic forces in diatom cell wall formation. In *Cytomechanics*, edited by J. Bereiter-Hahn, O. R. Anderson, and W-E. Reif, Springer-Verlag, Berlin **(1987)**, Vol. III.2, p. 183.
9. A.-M. M. Schmid, Aspects of morphogenesis and function of diatom cell walls with implications for taxonomy. *Protoplasma* 181, 43 **(1994)**.
10. D. G. Mann, *Shape and Form in Plants and Fungi*, edited by D. S. Ingram and A. J. Hudson, Academic Press, London **(1994)**, p. 17.
11. A-M. M. Schmid, R. K. Eberwein, and M. Hesse, Pattern morphogenesis in cell walls of diatoms and pollen grains: A comparison, *Protoplasma* 193, 144 **(1996)**.
12. E. Pfitzer, Untersuchungen über bau and entwicklung der bacillariaceen (Diatommen). In *Botanische Abhandlungen aus dem Gebiet der Morphologie und Physiologie* 1, 1 **(1871)**.
13. D. G. Mann, The species concept in diatoms. *Phycologia* 38, 437 **(1999)**.
14. J. D. MacDonald, On the structure of the diatomaceous frustule, and its genetic cycle. *Ann. Mag. Nat. Hist.* 4, 1 **(1869)**.
15. E. Pfitzer, Uber den bau and zellteilung der diatomeen. *Bot. Z.* 27, 774 **(1869)**.
16. L. Geitler, Der formwechsel der pennaten diatomeen. *Arch. Protistenkd.* 78, 1 **(1932)**.
17. E. F. Stoermer, Y.-Z. Qi and T. B. Ladewski, A quantitative investigation of shape variation in *Didymosphenia* (Lyngbye) M. Schmidt (Bacillariophyta). *Phycologia* 25, 494 **(1986)**.
18. J. L. Pappas and E. F. Stoermer, Multidimensional analysis of diatom morphologic and morphometric phenotypic variation and relation to niche. *Ecoscience* 2, 357 **(1995)**.
19. D. G. Mann, Why Lund didn't see sex in *Asterionella*? A discussion of the diatom life cycle in nature. In *Algae and the Aquatic Environment*, edited by F. E. Round, Biopress Ltd, Bristol **(1988)**, p. 384.
20. M. B. Edlund and E. F. Stoermer, Ecological, evolutionary, and systematic significance of diatom life histories. *J. Phycol.* 33, 897 **(1997)**.
21. J. A. Raven, The transport and function of silicon in plants. *Biol. Rev.* 58, 179 **(1983)**.

22. S. Mayama and A. Kuriyama, Diversity of mineral cell coverings and their formation processes: A review focused on the siliceous cell coverings. *J. Plant Res.* 115, 289 **(2002)**.
23. E. F. Stoermer, H. S. Pankratz and C. C. Bowen, Fine structure of the diatom *Amphipleura pellucida*. II. Cytoplasmic fine structure and frustule formation. *Am. J. Bot.* 52, 1067 **(1965)**.
24. B. E. Volcani, Cell wall formation in diatoms: Morphogenesis and biochemistry. In *Silicon and Siliceous Structures in Biological Systems*, edited by T. L. Simpson and B. E. Volcani, Springer-Verlag, New York **(1981)**, p. 157.
25. D. G. Mann, A note on valve formation and homology in the diatom genus *Cymbella*. *Ann. Bot.* 47, 267 **(1981)**.
26. D. G. Mann, Symmetry and cell division in raphid diatoms. *Ann. Bot.* 52, 573 **(1983)**.
27. D. G. Mann, *Hantzschia fenestrata* Hust. (Bacillariophyta)—*Hantzschia* or *Nitzschia*? *Br. Phycol. J.* 15, 249 **(1980)**.
28. F. E. Round, R. M. Crawford, and D. G. Mann, *The Diatoms: Biology and Morphology of the Genera*, Cambridge University Press, Cambridge, England **(1990)**.
29. H. G. Barber and E. Y. Haworth, *A Guide to the Morphology of the Diatom Frustule*, Freshwater Biological Association, England **(1981)**.
30. D. W. Kahn, *Topology*, Dover, New York **(1995)**.
31. K. Krammer and J. Lange-Bertalot, 3. Teil: Centrales, Fragilariaceae, Eunotiaceae. In *Süßwasserflora von Mitteleuropa, Band 2/3*, edited by H. Ettl, J. Gerloff, H. Heynig, and D. Mollenhauer, Gustav Fisher Verlag, Stuttgart, Germany **(1991)**.
32. K. Krammer and J. Lange-Bertalot, 2. Teil: Bacillariaceae, Epithemiaceae, Surirellaceae. In *Süßwasserflora von Mitteleuropa, Band 2/2*, edited by H. Ettl, J. Gerloff, H. Heynig, and D. Mollenhauer, Gustav Fisher Verlag, Stuttgart, Germany **(1988)**.
33. F. A. S. Sterrenburg, Studies on the genera *Gyrosigma* and *Pleurosigma* (Bacillariophyceae). Light microscopical criteria for taxonomy. *Diatom Res.* 6, 367 **(1991)**.
34. K. Krammer and J. Lange-Bertalot, 1. Teil: Naviculaceae. In *Süßwasserflora von Mitteleuropa, Band 2/1*, edited by H. Ettl, J. Gerloff, H. Heynig, and D. Mollenhauer, Gustav Fisher Verlag, Stuttgart, Germany **(1986)**.
35. D. DeCarlo and J. Gallier, Topological evolution of surfaces. In *Proceedings of the Twenty-eighth Graphics Interface Conference*, Toronto, Canada, A. K. Peters, Ltd. Natick, Massachusetts **(1996)**, p. 194.
36. J. D. Pickett-Heaps, Post-mitotic cellular reorganization in the diatom *Cymatopleura solea*: The role of microtubules and microtubule centre. *Cell Motil. Cytoskel.* 18, 279 **(1991)**.
37. A.-M. M. Schmid, Influence of environmental factors on the development of the valve in diatoms. *Protoplasma* 99, 99 **(1979)**.
38. K. H. Sandhage, M. B. Dickerson, P. M. Huseman, M. A. Caranna, J. D. Clifton, T. A. Bull, T. J. Heibel, W. R. Overton, and M. E. A. Schoenwaelder, Reactive conversion of diatom frustules: A novel, hybrid route to complex-shaped microstructures with tailored chemistries. *Adv. Mater.* 14, 429 **(2002)**.
39. M. Sumper, A phase separation model for the nanopatterning of diatom biosilica. *Science* 295, 2430 **(2002)**.
40. G. A. Ozin, Lamellar aluminophosphates that mimic radiolaria and diatom skeletons. *Nature* 378, 47 **(1995)**.
41. C. E. Hamm, R. Merkel, O. Springer, P. Jurkojc, C. Maier, K. Prechtel, and V. Smetacek, Architecture and material properties of diatom shells provide effective mechanical protection. *Nature* 421, 841 **(2003)**.
42. D. A. Forsyth, J. L. Mundy, V. di Gesú, and R. Cipolla, *Shape, Contour and Grouping in Computer Vision*, Springer-Verlag, Berlin **(1999)**.
43. C. M. Grimm and J. F. Hughes, Modeling surfaces of arbitrary topology using manifolds. In *Proceedings SIGGRAPH '95* **(1995)**, p. 359.
44. B.-Y. Chen, Y. Ono, H. Johan, M. Ishii, T. Nishita, and J. Feng, 3D model deformation along a parametric surface. In *Proceedings of IASTED International Conference on Visualization, Imaging and Image Processing* **(2002)**, p. 282.
45. M. Desbrun and M.-P. Cani-Gascuel, Active implicit surface for animation. In reply to: *Proceedings of Graphics Interface Conference*, Vancouver, Canada **(1998)**, p. 143.
46. C. H. Leung and M. Berzins, A computational model for organism growth based on surface mesh generation. *J. Comput. Phys.* 188, 75 **(2003)**.

Received: 30 May 2003. Revised/Accepted: 12 January 2004.